ELSEVIER

Journal of Nuclear Materials 307–311 (2002) 327–330

journal of nuclear materials

www.elsevier.com/locate/jnucmat

Effect of weld thermal cycle, stress and helium content on helium bubble formation in stainless steels

S. Kawano [a,*], F. Kano [a], C. Kinoshita [b], A. Hasegawa [c], K. Abe [c]

[a] *Power and Industrial Systems, R&D Center, Toshiba Corporation, 8 Shinsugita-cho, Isogo-ku, Yokohama 235-8523, Japan*
[b] *Faculty of Engineering, Kyushu University, 6-10-1, Hakozaki, Higashi-ku, Fukuoka 812-8581, Japan*
[c] *Faculty of Engineering, Tohoku University, Aramaki-aza-Aoba, Aoba-ku, Sendai 980-8579, Japan*

Abstract

Helium bubble structure was examined on a helium-implanted stainless steel after applying thermal and stress cycle using a weld thermal and stress cycle simulator. Helium ions were implanted on Type 304 stainless steels up to 200 appm uniformly to a depth of 3.5 μm. The specimens were heated at various temperatures between 1073 and 1473 K for 2 s in Ar gas atmosphere. Tensile stresses from 0.5 to 8 MPa were applied during the thermal cycle. TEM observations revealed that size of the bubbles at grain boundaries was larger for the specimens with a higher tensile stress and with a higher annealing temperature. Densities of bubbles increased with increasing helium content. A theoretical model calculation showed a good agreement with the experimental results.

1. Introduction

Degradation of weldability in neutron-irradiated stainless steels is one of the important issues for fusion reactor development and fission power reactor operation from the viewpoint of reactor maintenance. The reactor components exposed to high energy neutrons contain a large amount of helium produced by nuclear transmutation reactions. Helium is known to have a large effect on weldability and properties of welded joints [1–5]. The mechanism of weld cracking in irradiated materials is considered to be rapid growth of helium bubbles formed at grain boundaries (GBs) at high temperatures under the influence of thermal stresses, to a size sufficient to cause GB separation.

Some theoretical models of helium bubble behavior at GB during welding have been proposed to predict weldability [6,7]. In order to understand the mechanism of weld cracking in irradiated materials and verify the proposed models, it is necessary to know the details of bubble evolution during welding. In a previous study, the helium bubble structure was examined for helium-implanted stainless steels after applying thermal and stress cycle using a weld thermal and stress cycle simulator [8]. Helium bubble formation was observed in 304 stainless steels containing 5 appm He even after short annealing times and the size of the helium bubble at GBs was strongly dependent on the tensile stress during heating. In the present study, the effect of tensile stress, annealing temperature and helium content on the bubble formation is quantitatively examined for stainless steels implanted with helium ions up to 200 appm. The experimental results are compared with a theoretical model of helium bubble behavior during welding.

2. Experimental procedures

The material used is SUS304 stainless steel, with a grain size of about 20 μm. The chemical composition is: 0.06 C, 0.57 Si, 1.03 Mn, 0.025 P, 0.007 S, 8.57 Ni and 18.22 Cr in weight percent. Tensile specimens, the gauge sections of which were 14 mm long, 3 mm wide and 0.2 mm thick, were implanted with 3 MeV helium ions at room temperature. The implanted area was limited to

* Corresponding author. Tel.: +81-45 770 2372; fax: +81-45 770 2483.
E-mail address: shohei.kawano@toshiba.co.jp (S. Kawano).

0022-3115/02/$ - see front matter
PII: S0022-3115(02)01203-5

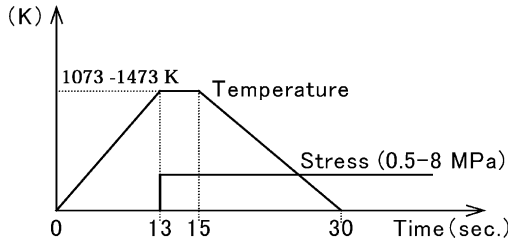

Fig. 1. Applied thermal and stress cycle.

3 mm in diameter at the center of the specimen. A beam energy degrader was applied to obtain a uniform helium-implanted layer which existed between 1.5 and 3.5 μm in depth from the surface. The calculated helium concentration was 50 and 200 atomic parts per million (appm).

The heat cycle was applied to the specimens by a weld thermal and stress cycle simulator [8]. Fig. 1 shows a schematic figure of the applied thermal and tensile stress cycle. The specimens were heated at various temperatures between 1073 and 1473 K for 2 s in Ar gas atmosphere. The heat-up rate and cooling rate were controlled to simulate temperature history at the position of HAZ during the tungsten inert gas welding at 20 kJ/cm heat input. Tensile stresses varying between 0.5 and 8 MPa were applied immediately after reaching the maximum temperature. Two cycle heating was also performed to investigate the effect of multi-cycle heating on the bubble behavior to multi-pass weld repair of reactor components. The specimens were re-heated at 1273 K with tensile stress of 2 MPa just after previous heating under the same condition was finished. After applying the thermal and stress cycle, TEM discs of 3 mm in diameter were punched out at the helium-implanted area of specimens. TEM discs were electropolished to the depth of 2 μm from the implanted surface and back-thinned for perforation in a 10% $HClO_4 + CH_3COOH$ solution. Microstructural observations were conducted using a TEM operated at 200 kV.

3. Calculation of helium bubble behavior

The helium bubble behavior at GBs during annealing tests was calculated based on a theoretical model [6,7] and compared with the microstructural observations. The model calculates bubble nucleation, coalescence and growth at the GB using the temperature and stress changes during the test. In the early stages of the heat-up period during the test, helium atoms in the grains are considered to diffuse to GBs and bubbles nucleate at GBs. Since a vacancy which holds up to two helium atoms (V-He_2) is assumed to be a bubble nucleus [7], the nucleation rate is given as the reaction rate of a vacancy-helium complex (V-He) and a helium atom,

$$\frac{dN}{dt} = f(K_{He} + K_{HeV})C_{He}C_{HeV}, \tag{1}$$

where N is the areal number density of GB bubble; f, the geometrical factor of the reaction; K_{He} and K_{HeV}, the reaction rate coefficients of He and V-He; C_{He} and C_{HeV}, the concentrations of helium atoms and V-He at GB respectively. C_{He} and C_{HeV} are determined by their flows into the GB, and thus the flow rate of helium atom and V-He into GB are calculated in the diffusion model respectively [7].

At elevated temperatures during heating, the bubble density on GBs decreases due to bubble coalescence along these boundaries [9]. The migration process of bubbles is considered to be random motion controlled by surface diffusion [10]. The time rate of change of the bubble density (N) on GBs is given by [6]

$$\frac{dN}{dt} = -\frac{2\pi a^4 D_s N^2}{r^4 \ln[1/(2r\sqrt{N})]}, \tag{2}$$

where D_s is the surface diffusion coefficient; r, the bubble radius and a, the lattice spacing. The average radius of coalesced bubbles is assumed to obey the conservation of volume [6].

During heating, the GB bubble is assumed to grow by thermal vacancy absorption due to helium gas overpressure in the bubble when applied stress is under 0, and to grow by stress-induced vacancy absorption when tensile stress is applied. The growth rate of bubbles is given [6] by

$$\frac{dr}{dt} = \frac{\delta\Omega D_{gb} C_v^e}{2r^2} \quad (\sigma \leqslant 0), \tag{3}$$

$$\frac{dr}{dt} = \frac{2\pi\delta\Omega D_{gb}\sigma\sqrt{N}}{rkT} \quad (\sigma > 0), \tag{4}$$

where r is the bubble radius; δ, the GB thickness; Ω, the atomic volume; D_{gb}, the self-diffusion coefficient in the GB; C_v^e, the equilibrium vacancy concentration; σ, the tensile stress normal to the GB; k, the Boltzmann constant; and T, the temperature. The calculations of bubble size and density were obtained by specifying $C_v^e = [\exp(1.5)\exp(-2\ \mathrm{eV}/kT)]/\Omega\ \mathrm{m}^{-3}$, $D_{gb} = 5 \times 10^{-5}\exp(-1.8\ \mathrm{eV}/kT)$ m/s. The other parameter values used in calculations were similar to these in [6,7].

4. Results and discussion

Fig. 2 shows TEM microstructures of the specimens containing 200 appm He after applying various thermal

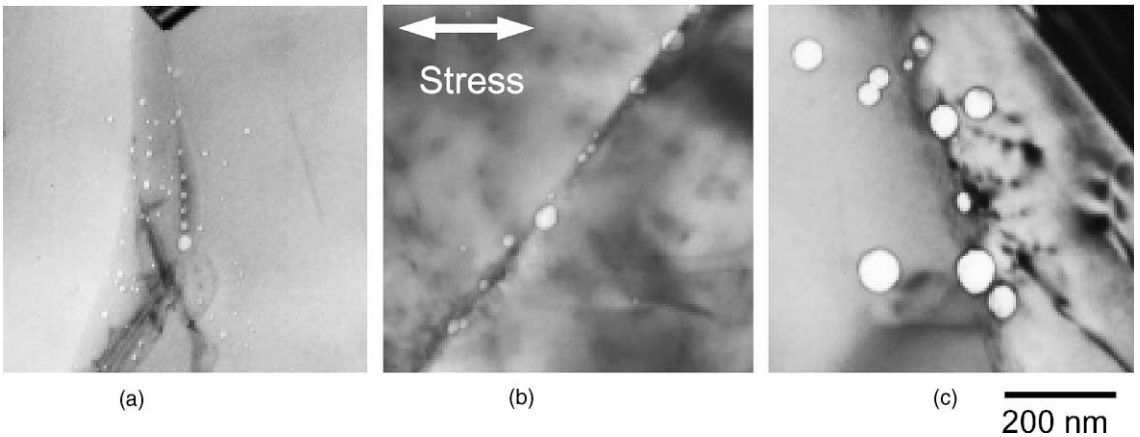

Fig. 2. Helium bubble microstructures in 200 appm He specimens after applying thermal and stress cycles: (a) 1073 K, 2 MPa, (b) 1273 K, 2 MPa, (c) 1273 K, 8 MPa.

and stress cycles. He bubbles were observed at GBs and in the matrix. Fig. 3 shows the average GB bubble diameter as a function of the angle between the stress direction and the GBs. The application of tensile stress during heating tends to increase the diameter of the bubbles located in GBs perpendicular to the applied stress. Fig. 4 shows the average diameter and density of bubbles observed in GBs perpendicular to the applied stress, together with theoretical calculations. The experimental data reveal that the bubble diameter was larger for the specimens with a higher annealing temperature and with a higher tensile stress. It is reported that tensile stresses during isothermal annealing tests enhance the bubble growth that is thought to be due to the vacancy absorption [11]. It is suggested that the GB bubble growth observed in this study is attributable to stress-induced vacancy absorption, which is often adopted in models for bubble growth during welding.

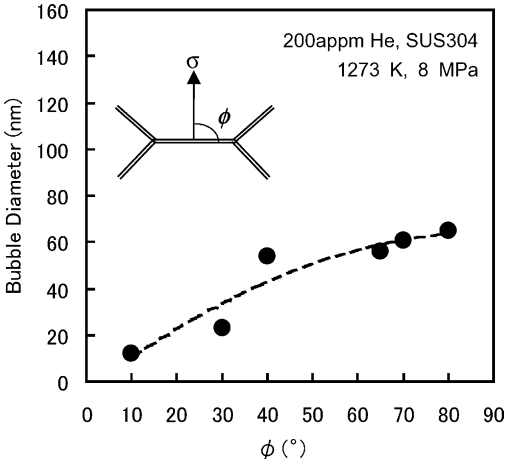

Fig. 3. Average helium bubble size as a function of the angle ϕ between the stress direction σ and the GB: 200 appm He, 1273 K, 8 MPa.

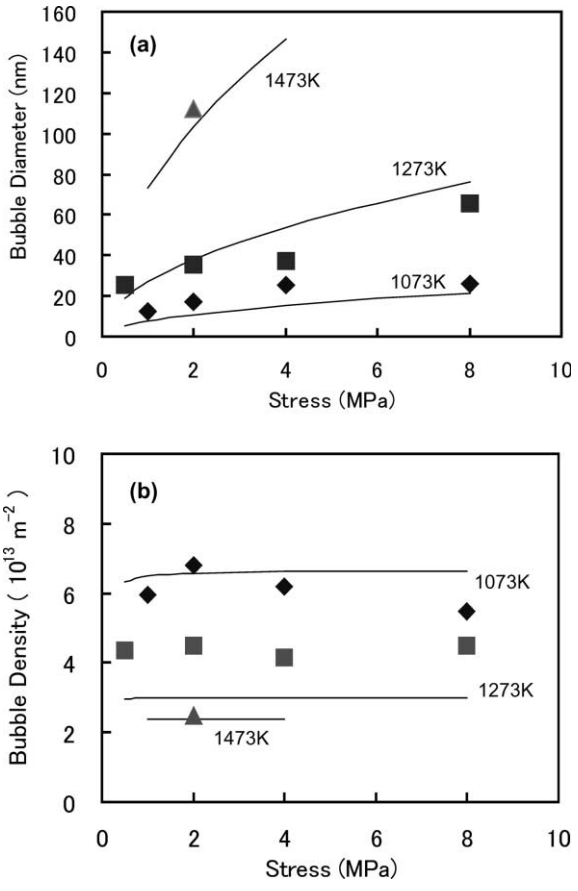

Fig. 4. The bubble diameter (a) and density (b) at GBs observed in 200 appm He specimens as a function of stress for different annealing temperatures. The curves show results of model calculations.

The observed bubble density decreased with increasing annealing temperature. It is considered that the bubble coalescence along these boundaries is enhanced at higher temperature due to the bubble migration controlled by surface diffusion. The calculated bubble size and density correspond well to the results of TEM observations in this study.

Fig. 5 shows the GB bubble diameter and density obtained from TEM observations as a function of helium content, together with theoretical calculations. The observed bubble diameter and density increased with helium content. The bubble nucleation at GB is considered to be increased by increasing the flow of helium atoms into GB in the specimen with higher helium content. The calculated results are in good agreement with the results of TEM observations. Fig. 6 shows the effect of applied thermal/stress cycle number on GB bubble diameter and density. Applying two thermal cycles enhances the bubble growth. Theoretical calculations can hence predict the bubble behavior in various thermal/stress cycles.

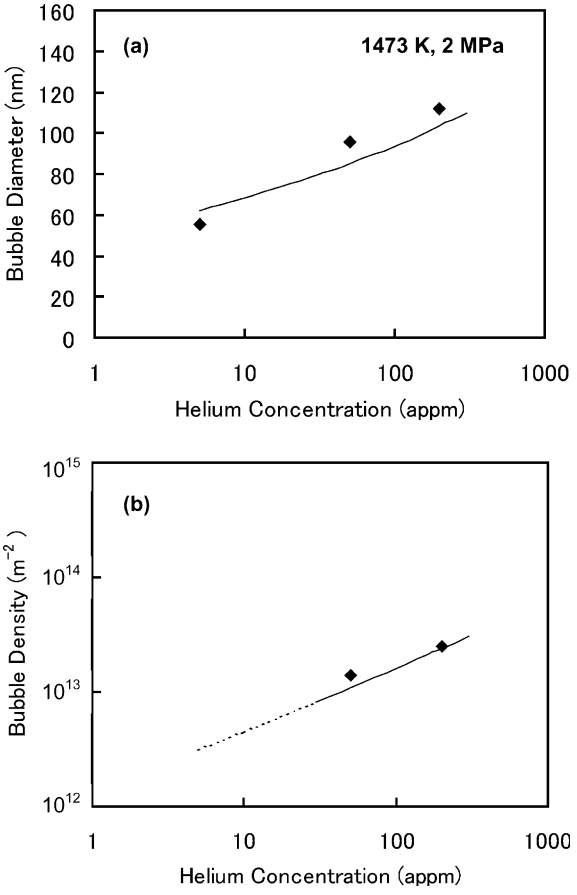

Fig. 5. GB bubble diameter (a) and density (b) from TEM observations as a function of helium concentrations. The curves show results of model calculations: 1473 K, 2 MPa.

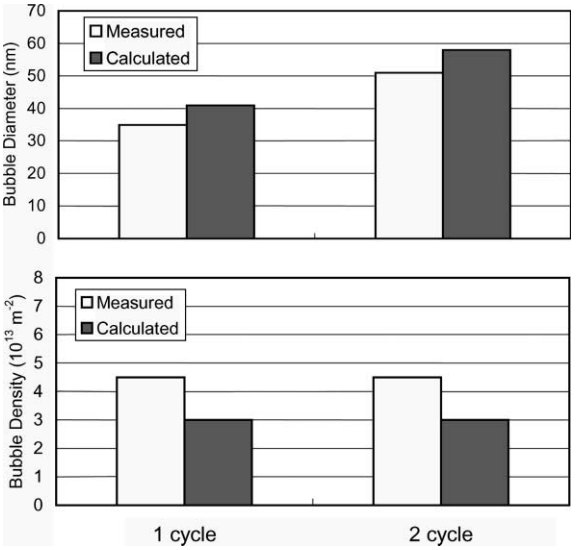

Fig. 6. Effect of applied thermal/stress cycle number on GB bubble diameter and density in the case of 200 appm He specimen: 1273 K, 2 MPa.

5. Conclusions

The helium bubble structure was examined in helium-implanted 304 stainless steels after applying thermal and stress cycle using a weld thermal and stress cycle simulator. TEM observations revealed that size of the bubbles at GBs was larger for the specimens with a higher tensile stress and with a higher annealing temperature. Densities of bubbles increased with increasing helium content. A theoretical model calculation showed a good agreement with the experimental results.

References

[1] W.R. Kanne Jr., Welding J. 67 (1988) 33.
[2] W.R. Kanne Jr., G.T. Chandler, D.Z. Nelson, E.A. Franko-Ferreira, J. Nucl. Mater. 225 (1995) 69.
[3] C.A. Wang, M.L. Grossbeck, N.B. Potluri, B.A. Chin, J. Nucl. Mater. 239 (1996) 85.
[4] K. Asano, S. Nishimura, Y. Saito, H. Sakamoto, Y. Yamada, T. Kato, T. Hashimoto, J. Nucl. Mater. 264 (1999) 1.
[5] H.T. Lin, M.L. Grossbeck, B.A. Chin, Metal. Trans. A 21 (1990) 2585.
[6] S. Kawano, R. Sumiya, K. Fukuya, J. Nucl. Mater. 258–263 (1998) 2008.
[7] T. Hashimoto, M. Mochizuki, ASTM 1366 (2000) 973.
[8] S. Kawano, K. Fukuya, F. Kano, M. Satou, J. Nucl. Mater. 283–287 (2000) 1220.
[9] S.H. Goods, N.Y.C. Yang, Metal. Trans. A 23 (1992) 1021.
[10] A. Ryazanov, D. Braski, H. Schroeder, H. Trinkaus, H. Ullmaier, J. Nucl. Mater. 233–237 (1996) 1076.
[11] H. Trinkaus, H. Ullmaier, Philos. Mag. 39 (1979) 563.